

Received March 3, 2018, accepted March 28, 2018, date of publication April 10, 2018, date of current version May 24, 2018.

Digital Object Identifier 10.1109/ACCESS.2018.2825224

A Method for 3-D Printing Patient-Specific Prosthetic Arms With High Accuracy Shape and Size

JOHN-JOHN CABIBIHAN¹, (Senior Member, IEEE), M. KHALEEL ABUBASHA², AND NITISH THAKOR^{3,4}, (Life Fellow, IEEE)

¹Department of Mechanical and Industrial Engineering, Qatar University, Doha, Qatar

²Department of Mechanical Engineering, Texas A&M University, College Station, TX 77843, USA

³Singapore Institute of Neurotechnology, National University of Singapore, Singapore 117456

⁴Department of Biomedical Engineering, Johns Hopkins University, Baltimore, MD 21205, USA

Corresponding author: John-John Cabibihan (john.cabibihan@qu.edu.qa)

This work was supported by the NPRP Grant from the Qatar National Research Fund under Grant NPRP 7-673-2-251. The statements made herein are solely the responsibility of the authors.

ABSTRACT Limb amputation creates serious emotional and functional damage to the one who lost a limb. For some upper limb prosthesis users, comfort and appearance are among the desired features. The objective of this paper is to develop a streamlined methodology for prosthesis design by recreating the shape and size of an amputated arm with high accuracy through 3-D printing and silicone casting. To achieve this, the computer tomography (CT) images of the patient's affected and non-affected arms were scanned. Next, the geometry of the socket and the prosthetic arm were designed according the mirrored geometry of the non-affected arm through computer-aided design software. The support structure and the moulds were 3-D printed, and the prosthetic arm was casted with a silicone material. To validate the replication, the shape of the socket and prosthetic arm were quantitatively compared with respect to the source CT scan from the patient. The prosthetic arm was found to have high accuracy on the basis of the Dice Similarity Coefficient (DSC; 0.96), percent error (0.67%), and relative mean distance (0.34 mm, $SD = 0.48$ mm). Likewise, the socket achieved high accuracy based on those measures: DSC (0.95), percent error (2.97%), and relative mean distance (0.46 mm, $SD = 1.70$ mm) The liner, socket, and prosthetic arm were then shipped to the patient for fitting. The patient found the fit of the socket and the replication of the shape and the size of the prosthesis to be desirable. Overall, this paper demonstrates that CT imaging, computed-aided design, desktop 3-D printing, and silicone casting can achieve patient-specific cosmetic prosthetic arms with high accuracy.





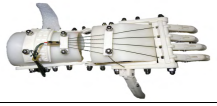


INDEX TERMS 3-D printing, prosthetics, computer tomography imaging, assistive technologies, social implications of technology.

I. INTRODUCTION

The World Health Organization estimates that individuals with physical disabilities who need prosthetics or orthotic devices represent 0.5% of the population [1], [2]. With the combined population of Asia, Africa, Latin America, and the Caribbean to be around 6.3 billion at this time [3], those who need such devices in the developing countries are estimated to be around 31 million individuals. In addition to this, the recent wars in some parts of the world have resulted in another 1 million injured people and around 8% of them need prostheses or orthoses [4]. This equates to around 80,000 additional individuals who need such devices to help them in their day-to-day activities.

The cost of upper limb prosthetics that are being developed for industrialized countries is quite high by global standards. The price of body-powered prostheses range from \$4,000 to \$50,000, while the price of the externally-powered ones cost from \$25,000 to \$50,000 [5]. A sudden shift in the cost to produce prosthetic devices can be attributed to the expiry of the first patent on Fused Deposition Manufacturing (FDM) in 2007 [6]. Since then, we have seen a wide availability of consumer-grade desktop three-dimensional (3D) printers, which cost around \$250 to \$2,500. 3D printing is the layer-by-layer deposition of material to construct parts from a 3D computer graphics model [7]. There have been rapid applications of 3D printers for electronics manufacturing [8]–[10]

TABLE 1. 3-D Printed prosthetic hands

Robot Hand's Name, Company, Organization or Designer	Prosthetic Hand Design	Actuation Type	Human Hand-like Shape?	Patient-Specific Size?
Cyborg Beast, Univ. of Nebraska Omaha, Dept. of Biomechanics		Body-Powered	No	No
Raptor Hand, e-Nable community		Body-Powered	No	No
FlexyHand, Gyrobot, LLC, Swindon, UK		Body-Powered	Yes	No
K1 Hand, Evan Keuster, 3D Systems, SC, USA		Body-Powered	No	No
Robohand, Richard Van As		Body-Powered	No	No
Handiii Coyote, exiii, Inc., Tokyo, Japan		Myoelectric	Yes	No
Ada Hand, Open Bionics, LLC, Bristol, UK		Mechatronic	Yes	No

and biomedical engineering [11]–[13], among others. The ubiquity of 3D printers has democratized the manufacturing of prosthetics for augmenting physical disabilities [14]. Upper limb prosthetics can now be produced with the cost of production ranging from \$300 to \$2,000.

In a survey on 242 upper limb amputees [15], the participants selected fit, lifelike appearance, cost, and color as the highest design priorities for passive artificial hands. For electric hands, the participants selected glove durability, cost, sensory feedback, and lifelike appearance. For body-powered hooks, they selected comfort, cost, movement, grip strength, and fit. One of the key findings of that survey is the amputees' demand for a more natural, lifelike appearance for those using either passive or electric prosthetic hands. For body-powered hooks, increased comfort on the harness or strap was the highest priority.

The more commonly-available 3D printed designs are for body-powered prostheses for below-elbow upper limb amputation. The 3D printed design approach was made possible due to the open access movement in various communities [16], [17]. To determine the sizes of the prosthetic hands, the designers request photographs of the affected and non-affected parts of the amputee's arm. Software (e.g. Blender software) is used to approximate the size of the prosthetic arm relative to the missing arm. The prosthetic

arm design is then 3D printed and sent to the patient. For the electric powered prosthetic hands, users select available sizes online (i.e. small, medium, large). The motors and the actuation system are typically built into the structure; thus, approximating the hand size of the patient requires additional design effort. Lastly, passive prosthetic hands are being constructed by getting the amputee to immerse his/her non-affected hand in an alginate mixture (e.g. Alja-Safe, Smooth-On Inc, PA, USA) to get a negative mould of the hand. Silicone rubber is used to get a cast of the desired shape. The constructed part is then 3D scanned. Solid modeling software (e.g. SolidWorks, CATIA) is used to get a mirror image of the desired hand, which is then 3D printed for the amputee [18], [19].

In an earlier study where 3D printed upper limb prosthetics were reviewed [5], it was reported that the users desired the following features: anthropomorphic appearance, functionality, comfort, and durability. Some examples of 3D printed prosthetic hands are shown in Table 1. In Arabian *et al.* [20], prosthetic hand designs were shown to 14 amputees in Jordan and Haiti (the first 4 3D printed hands in Table 1). After selection, the authors printed the selected prosthetic hands and fitted these to the participants. They found that the selected 3D printed prosthetic hands did not meet the aesthetic expectations of the amputees even for the hands

that were initially seen to be desirable in the photographs. Additionally, the cultural backgrounds of the participants that were selected were said to be more aesthetically sensitive. Thus, the 3D printed prosthetic hands were rejected.

Murray [21] stated that the use of prosthesis plays a social role where the use of prosthetics help ward off the social stigma that is associated to the loss or absence of limbs. Rather than conceal the usage of prosthesis, the current designs of 3D prosthetic hands attracted attention. Current 3D printed prosthetic hands still do not fully address the desired requirements of the amputees. An appealing look of a prosthetic hand should include the mimicry of the general aspects of the human hand [22]–[25]. The prerequisite features are lifelike shape, size, color, and aesthetic details (e.g. pores, hair, etc). The industry for the rehabilitation of upper limbs and the movie-making industry have generated impressive results in replicating color and fine details [26], [27].

This paper presents a technique to construct patient-specific upper limb prosthetics with high accuracy shape, along with the size to replicate a patient's missing arm. Moreover, the method does not require the physical presence of an amputee for measurements and for the design process. The next section describes a procedure to replicate the missing arm using the mirrored version of the non-affected arm using computer tomography (CT) images. The socket, moulds, and the supporting structures were designed using computer-aided design methods. We elaborate the process where the moulds were 3D printed and silicone material was casted on it to replicate the shape and size of the missing limb. Section III presents the quantification of the replication accuracy. Lastly, Section IV discusses the potential of this technique for affordable lifelike prosthetics and concludes the work.

II. MATERIALS AND METHODS

A. PARTICIPANT

A 26-year old woman underwent an amputation due to a car accident. The amputation below the elbow of the left arm was immediately performed after the accident. The residual limb was about 93 mm in length measured from the elbow joint's crease. Regular dressing was applied to the stump. The stump healed after three months.

The patient completed the self-report module on Orthotics and Prosthetics Users' Survey (OPUS) Quality of Life Index [28]. On the question on "How much does your physical condition restrict your ability to do paid work?", the patient replied "excessively". For all the questions below, the patient's reply was "a great deal".

- How much do you keep to yourself to avoid people's reactions to a missing body part or your need for a device?
- To what extent do you accomplish less than you would like because of your physical condition?
- How much does your physical condition restrict your ability to run errands?

- How much does your physical condition restrict your ability to pursue a hobby?
- How much does your physical condition restrict your ability to do chores?
- To what extent have you cut down on work or other activities because of your physical condition?

The attending clinician recommended a prosthesis for improving appearance and for accomplishing the tasks of daily living. Through email communications to the design team, the patient expressed her initial need for a cosmetic prosthetic arm due to the cost considerations for a more advanced prosthesis.

B. ETHICS

The procedures for this work did not include invasive or potentially hazardous methods and were in accordance with the Code of Ethics of the World Medical Association (Declaration of Helsinki). Written informed consent was granted by the patient for the publication of the CT images and photographs. The patient also agreed to the sharing of the CT scan data of her arm to be made available for research purposes.

C. DATA ACQUISITION

To acquire data for the design of the prosthetic arm, CT images were taken from the patient's affected and non-affected arms. The patient's data were acquired with a helical CT scanner (Somatom Definition AS, Siemens, Germany) at a hospital in Kampala, Uganda. The scanning parameters that were selected were: 130 kV, 70 mA, 0 gantry tilt, and 1 mm per second image slice thickness. The CT images were saved as Digital Imaging and Communications in Medicine (DICOM) format. The patient asked someone to send the CT scan data to the design team through cloud storage services. The DICOM files were imported to Mimics Innovation Suite (v19, Materialise, Belgium) for image processing and visualization of the patient's data in 3D geometry. The various anatomical views of the affected and affected arms are shown in Fig. 1a and 1b, respectively.

For validation purposes, another set of CT images (Fig. 1c) were taken after the prosthetic arm was constructed to compare the participant's arm and the replicated arm. The constructed prosthetic arm was scanned with a helical CT scanner (Somatom Drive, Siemens, Germany) at a hospital in Doha, Qatar. The scanning parameters were as follows: 120 kV, 60 mA, 0 gantry tilt, and 1 mm per second image slice thickness.

Alternatively, the patient's data can be acquired from portable 3D scanners. In terms of accuracy, portable 3D scanners (e.g. Eva, Artec3D, Luxembourg) and CT scanners can both provide resolutions below 1 mm, which is suitable for lifelike prosthesis. On the practical side, patients from low-resource countries may not have access to portable 3D scanners. The lowest priced models cost around \$10,000. In comparison, hospitals already provide CT imaging

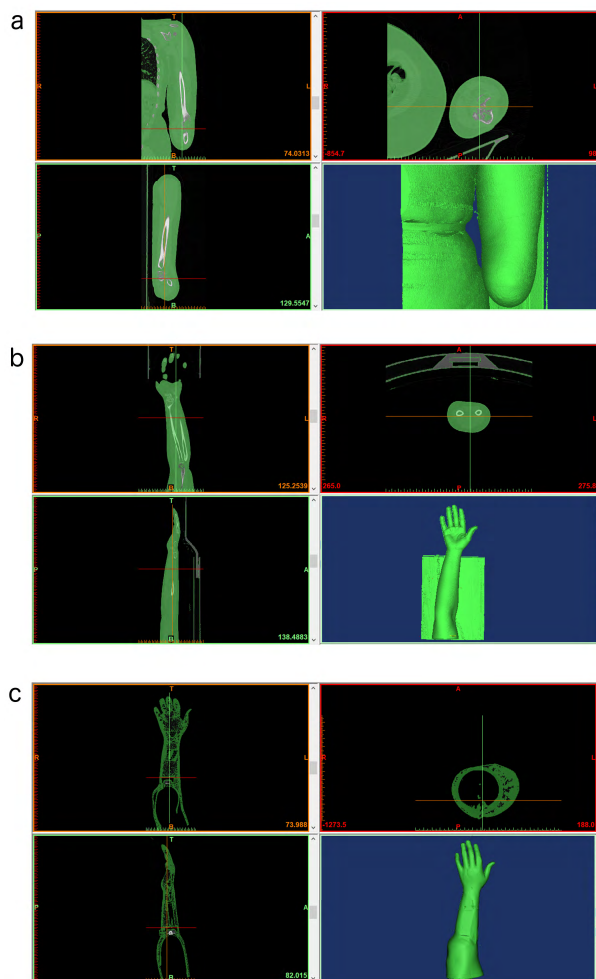


FIGURE 1. Computer Tomography (CT) images. (a) Amputated left arm. (b) Uninjured right arm. (c) Prosthetic arm. Each set of data are visualized according to the following views: coronal or the front view (top left); axial or the top-to-bottom view (top right); sagittal or the right side view (bottom left) and 3D model reconstruction (bottom right).

services and a body scan costs around \$350. For our purposes, obtaining the patient's measurements using a CT scanner was more appropriate.

D. DESIGN AND FABRICATION PROCESS FOR THE PROSTHETIC ARM

The patient's CT data were imported to a 3D modeling software (3-Matic, v10.0, Materialise NV, Leuven, Belgium) for visualization and editing (Fig. 2a and 2b). This was valuable to develop the design strategy for the replication of the arm's geometry. The software was used to create a mirror image of the right arm to the left arm (Fig. 2c). To obtain an accurate anatomic position of the missing left forearm, the remaining radius and ulna bones were used as reference markers for the mirrored left forearm.

A structural support was designed (Fig. 2d) to prevent the arm from being excessively deformable after the casting of the silicone material. Additionally, this part served as a

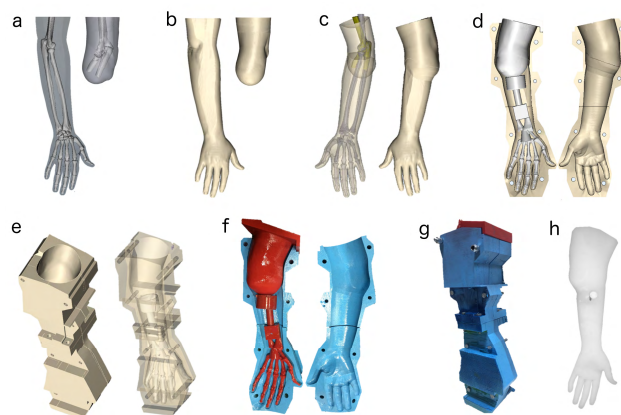


FIGURE 2. Design and fabrication process for the prosthetic arm. (a) The affected and non-affected arms of the patient in a semitransparent view. (b) 3-D surface reconstruction of the CT scan images. (c) Mirrored right arm aligned with the left limb according to the anatomic position of elbow joint, and the ulna and radial bones. (d) A 3-D reconstruction of the arm was done. (e) The four-part model of the mould where the bones were substituted with a single supporting structure. The assembled model of the mould design showing the cavity for pouring the liquid silicone material. (f) The 3-D printed models of the mould. After the liquid silicone cures, the cup-like part (in red) is detached to position the socket. (g) The assembled mould fixed by bolts and nuts. (h) The volar side of the fabricated prosthetic arm.

structural support for the fingers. For this support structure, it was not necessary to replicate the radius and ulna bones. Hence, a single shaft was designed. Fig. 2e shows the four-part computer model of the mould, which allowed us to create a one-piece arm with the build volume limitations of a desktop 3D printer (Replicator 5th Generation, Maker-Bot Industries LLC, Brooklyn, NY, USA; $29.5 \times 19.5 \times 16.5 \text{ mm}^3$).

The 3D printed skeleton of the hand, the arm, and the four-part split mould are shown in Fig. 2f. The assembled mould and skeleton structure are shown in Fig. 2g with bolts and nuts to fix them in place. The mould provides a cavity for the liquid silicone material (Dragonskin, Smooth-On Inc, PA, USA) to be poured. The silicone cured after 24 hours at room temperature. The prosthetic arm is shown in Fig. 2h. It took 5 days to complete the prototype. The cost of the expended filament and the silicone material is around \$20. Henceforth, we will refer to the mirrored version of the uninjured arm as the patient's arm.

E. DESIGN AND FABRICATION PROCESS FOR THE SOCKET

The socket serves as the interface between the prosthetic arm and the stump (i.e. the remaining part of the amputated limb). Analogous to wearing socks, the patient wears a liner (Icecross, item I-012426.5, Össur, Reykjavik, Iceland) before wearing the socket. A shuttle lock mechanism (Icelock 600 series, item L-621000, Össur, Reykjavik, Iceland) was then selected to connect the socket to the prosthetic arm. The main goals for the design and fabrication of the socket are firstly, to achieve functional movement of the elbow and secondly, to achieve comfort when the socket is worn. For the

requirement of providing functional movements, the range of motion was considered for the flexion and extension of the elbow and to design the socket to allow unconstrained movements. For the requirement on comfort, the socket needs to have a snug fit on the stump so as to prevent the prosthetic arm from falling off.

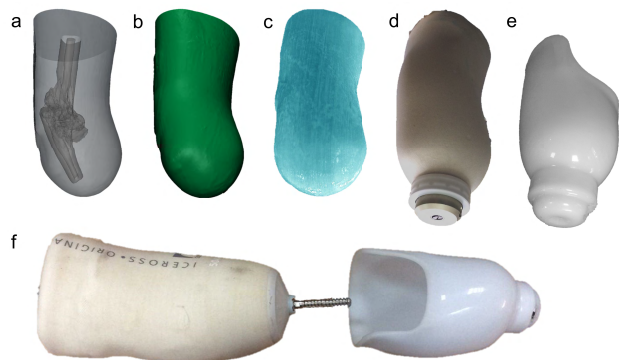


FIGURE 3. Design and fabrication process for the socket. (a) The stump, in a semitransparent view, showing the elbow joint. (b) A graphical model of the stump. (c) 3-D printed model of the stump. (d) The model of the stump with the shuttle lock mechanism. (e) The fabricated socket. (f) The assembly of the liner and the socket. The threaded part at the liner’s tip will pass through the socket and will connect this assembly to the prosthetic arm.

The stump and the elbow joint can be visualized from the semitransparent view of the patient’s amputated arm in Fig. 3a. This requires that the socket design needs to have a U-shaped opening at the elbow joint at around 60 mm distance from the tip of the stump for flexion and extension. The CT data in DICOM format were converted to stereolithographic (STL) file format (Fig. 3b). Using the data from this file, the arm was then 3D printed (Fig. 3c) to physically recreate the patient’s stump for fabricating the socket. The 3D printer used was a relatively low-cost desktop printer (Replicator 5th Generation, MakerBot Industries LLC, Brooklyn, NY, USA). The printing resolution of the machine is 0.1 mm.

Combined with the 3D printed model of the stump, the socket was fabricated using traditional methods [29], [30]. A positive mould of the stump (Fig. 3d) was created to attach the ratchet. The mould was constructed using gypsum powder (Qatar Gypsum Products Factory, Doha, Qatar). With the mould replicating the stump’s shape and the shuttle lock mechanism in place, a soft, flexible, and washable material was selected for the socket (Fig. 3e; Thermolyn Supra, item 616T111 = 9, Otto Bock Healthcare, Duderstadt, Germany). The material was heated in an oven to 175°C temperature. After heating, the material was moulded to the cast and was allowed to cool at room temperature. This resulted to a socket with high surface quality. The whole fabrication process for the socket took 1 day to complete as this is a standard process in prostheses and orthoses fabrication. The assembly of the liner and the socket is shown in Fig. 3f. The patient will wear the liner. The threaded part at the liner’s tip will be inserted through the socket. The thread will then lock the prosthetic

arm in place. The total cost of the mechanism, expended 3D printer filament, and materials is around \$960.

F. EVALUATION FOR THE PART ACCURACY

To evaluate the geometric accuracy of the constructed prosthetic arm and the socket, the CT scanned images were compared with the CT data from the patient. This process required that the models were digitally superimposed with one another. The models were geometrically matched using the Global Registration feature of the design software (3-Matic, v10.0, Materialise NV, Leuven, Belgium). Since the calculations only required that the external geometries are compared, all the spaces occupied by the bone and internal structures were filled up in the computer model.

Three similarity measures were used. First, the Dice Similarity Coefficient (DSC) was employed. Also known as the coefficient of association, this measure shows how two entities overlap [31]. This overlap can be obtained by using a Boolean intersection operation between two part models. The DSC was calculated as:

$$DSC = \frac{2|V_1 \cap V_2|}{|V_1| + |V_2|} \tag{1}$$

where V_1 is the part volume from the patient’s CT data and V_2 is the part volume from the prosthetic arm or the socket. A DSC of 1 shows that the two geometries are identical.

The second similarity measure is the percent error, which is the difference between the mirrored CT scan data from the unaffected arm of the patient and the prosthetic arm or the socket as a percentage of the CT scan data from the unaffected arm. This can be seen as the excess material. Percent error was calculated as:

$$\%Error_{arm} = \frac{|V_1 - V_2|}{V_1} \times 100 = \frac{|V_3|}{V_1} \times 100 \tag{2}$$

$$\%Error_{socket} = \frac{|V_1 \cap V_2|}{V_1} \times 100 = \frac{|V_3|}{V_1} \times 100 \tag{3}$$

where V_1 is the volume of the mirrored image of the patient’s data and V_2 is from the prosthetic arm or the socket. V_3 is the volume of the excess material from either the prosthetic arm or the socket. For the prosthetic arm, the Boolean subtraction operation was done for the volume of the uninjured arm versus the volume of the prosthetic arm. For the socket, the Boolean intersection operation was done to obtain the spatial overlap between the volume of the stump and the socket. A small percent error indicates close similarity between the two parts that are being compared.

The last similarity measure is based on distance measurements, where the relative distances of the geometric elements of the prosthetic arm were compared with the human arm. A part comparison analysis was done using 3-Matic (v10.0, Materialise NV, Leuven, Belgium). The software calculates the point-by-point descriptive statistics for central tendency (mean and median) and dispersion (standard deviation, minimum and maximum values).

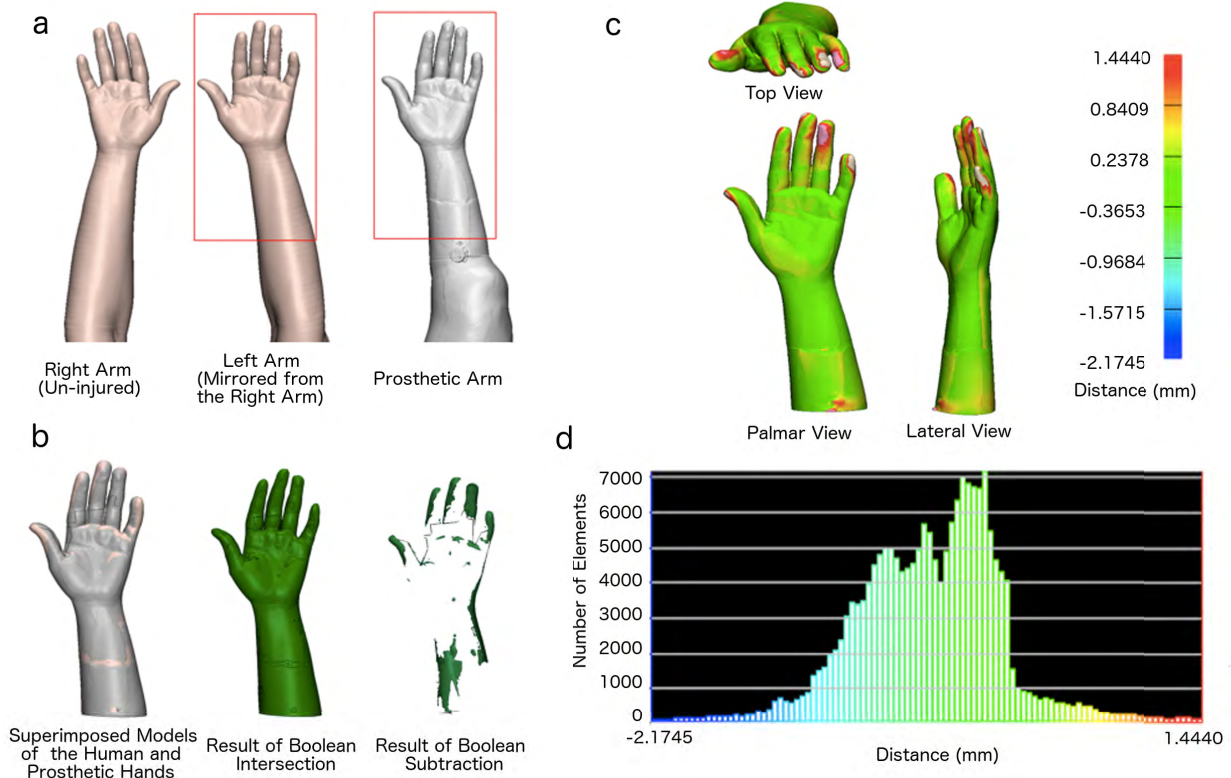


FIGURE 4. Comparisons between the mirrored image of the patient’s arm and the prosthesis. (a) The patient’s non-affected arm and its mirror image, together with the CT scan data of the prosthetic arm. The region of interest for comparisons is in red (b) The human and prosthetic hands when superimposed with each other. Shown are the results of Boolean intersection and subtraction operations. (c) Part comparisons showing the various views. The color bar indicates that the maximum distance of the prosthetic arm model from the human arm model are shown to be 1.44 mm (red) and the minimum to be 2.17 mm (blue) (d) Histogram of the part comparison analysis showing the distribution of the number of elements and the relative distance of the prosthetic arm from the human arm.

III. RESULTS

The geometry of the prosthetic arm and the socket were quantitatively compared with respect to the CT scan from the patient. The liner, socket, and prosthetic arm were then shipped to the patient for fitting for the evaluations for comfort and appearance.

TABLE 2. Volume data for the arm and the socket.

	Arm	Socket
Patient’s Data (cm ³)	813.79	306.48
Prosthesis (cm ³)	817.19	319.46
Cavity (cm ³)	-	195.03
Intersection (cm ³)	779.91	296.93
Boolean Operation (cm ³)	5.46	9.09

A. PROSTHETIC ARM ACCURACY

The prosthetic arm was designed according to the mirrored geometry of the non-injured arm. To determine the accuracy of replicating the non-affected arm, we selected the region of interest (ROI) in Fig. 4a. The region near the socket can be neglected due to the additional material. Table 2 shows the volume data collected for the arm and socket models for the

TABLE 3. Calculated and measured quantities of the similarity indicators for the arm and socket.

	Arm	Socket
Dice Similarity Coefficient	0.96	0.95
Percent Error (%)	0.67	2.97
Minimum, Maximum (mm)	-2.17, 1.44	-4.41, 5.07
Mean ±Std Dev (mm)	-0.34 ±0.48	-0.46 ±1.70
Median (mm)	-0.32	-0.35

patient and for the constructed prosthesis. Table 3 provides the calculated and measured sets of data using DSC, percent error, and distance measurements.

The model of the patient’s arm has a volume of 813.79 cm³ while the prosthetic arm has a volume of 817.19 cm³. For the calculation of the DSC (Eqn. 1), both models were superimposed (Fig. 4b). The Boolean intersection operation was done to obtain the shared volume between the two models. This resulted into a volume of 779.91 cm³. The proposed method shows a high DSC value of 0.96 (Table 3), which implies that the prosthetic arm is in close agreement with the mirrored image of the patient’s injured arm.

To know where the errors came from, we used a Boolean subtraction operation to investigate the excess material

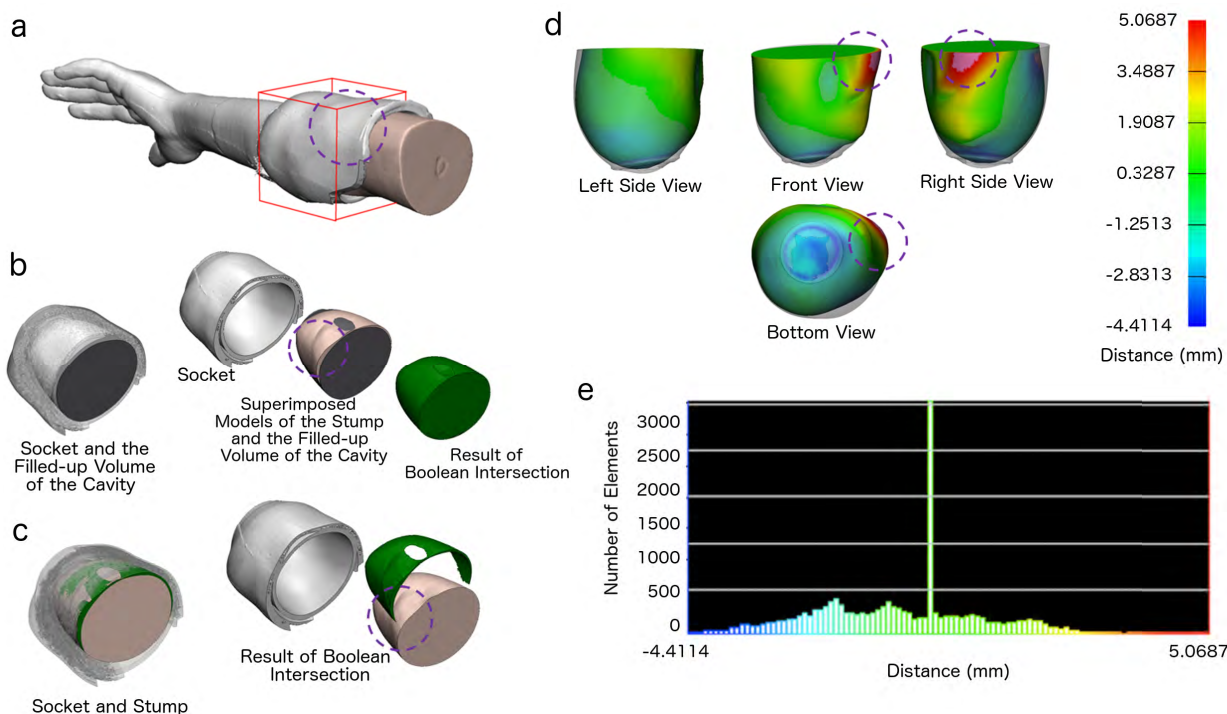


FIGURE 5. Comparisons between the participant's stump and the socket. (a) Visualization of the prosthetic arm and the socket showing the region of interest socket (red). Encircled (purple) is the reference location for the elbow. (b) The socket (light gray) and the construction of a new part model to represent the volume occupied by the cavity (dark gray). The patient's stump (light brown) was superimposed with the new part to represent the cavity. The Boolean intersection operation is shown (green). (c) The stump (light brown) was aligned with the socket. The exploded view shows the result of the Boolean intersection operation for the overlapping material (green). (d) Part comparisons showing the various views. The color bar indicates that the stump overlapped with the socket by 5.07 mm (red) and the stump was smaller than the socket by a distance of 4.41 mm (blue). (e) Histogram of the part comparison analysis showing the distribution of the number of elements and the relative distance of the prosthetic socket from the stump. Majority of the elements can be found at the zero distance because the volume of the stump and the socket were superimposed and were directly overlapping; thus there was zero difference in distance.

between the prosthetic arm and the patient's CT model of the mirrored image of the non-affected arm. The Boolean subtraction yielded a difference of 5.46 cm³. The excess material, which was represented as a percent error (Eqn. 2), is equivalent to 0.67%. The excess materials were mostly at the distal parts of the fingers (Fig. 4c).

A part comparison analysis feature of the software was conducted to determine the various distance measurements of the prosthesis in comparison to the CT data of the human arm. The various representative views of the prosthetic arm model show the locations of the excess material (Fig. 4c). The region shown in red shows the maximum distance of the prosthetic arm from the human arm (i.e. the prosthesis is slightly larger than the human arm). The distal phalanges of the thumb, index, and little fingers show the largest distance to be 1.44 mm. The negative distance of -2.17 mm implies that there are elements (i.e. data points) from the prosthetic arm that are smaller than the elements from the human arm. Fig. 4d shows the chart showing the number of elements and the corresponding distance between the prosthetic arm and the human arm. The mean distance is -0.34 mm (*SD* = 0.48 mm) while the median distance is -0.32 mm.

B. SOCKET ACCURACY

Similar to the prosthetic arm, the prosthetic socket and the stump were quantitatively compared using DSC, percent error, and the distance measures (Table 1). The ROI for the analysis of the socket's replication accuracy was determined to be the region below the U-shaped opening for the elbow flexion and extension (Fig. 5a; also refer to Fig. 3f). This was approximately located at a measurement distance from the tip of the socket up to 60 mm linear length.

The shared volume between the two part models were necessary to calculate the DSC (Table 2). Thus, a new part was created to fill up the open cavity of the socket (Fig. 5b). A Boolean intersection operation was done for us to inspect the volume where this new part intersected with the patient's stump. With the patient's stump having a volume of 306.48 cm³ and the cavity's volume to be 319.46 cm³, the DSC was calculated to be 0.95 (Table 3). This suggests that the fabricated socket will be able to accommodate the patient's stump due to the high similarity in the space that they both occupy.

To determine the locations where there are high errors or differences, we determined where the volume of the patient's stump overlapped with the socket. Thus, the Boolean

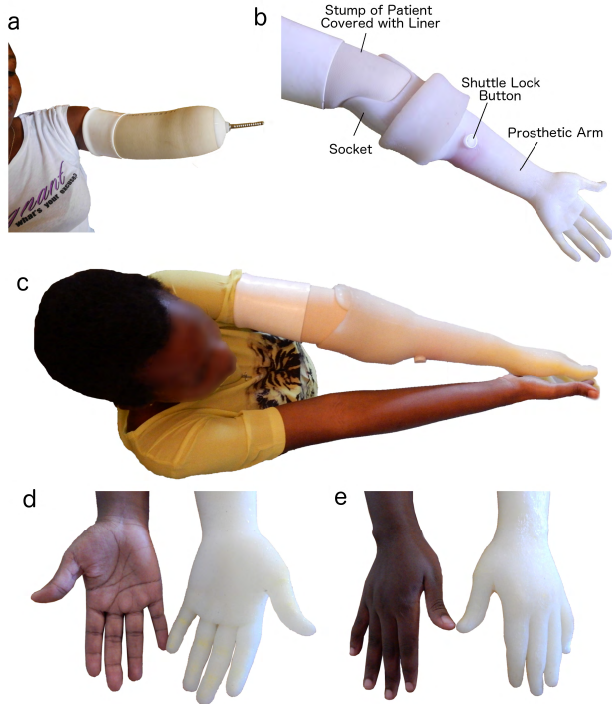


FIGURE 6. Fitting of the prosthesis liner and the comparisons between the non-affected arm and the prosthesis. (a) The patient wearing the liner. The threaded insert on the liner passes through the socket to lock the prosthetic arm in place. (b) The liner, socket, and prosthetic arm assembly. To detach the prosthetic arm, the shuttle lock button has to be pressed. (c) The participant comparing the length of the prosthetic arm to her unaffected arm. Shape and length comparisons (d) at the volar and (e) dorsal sides of the hand.

intersection operation was done (Fig. 5c). With the patient's stump (light brown) having a volume of 306.48 cm^3 and the socket's volume (light gray) to be 319.46 cm^3 , the intersection volume was 9.09 cm^3 (green). This represents a 2.97% error in volume of the stump that overlapped to the socket (Eqn. 3).

The part comparison analysis (Fig. 5d) shows a maximum distance of 5.07 mm and a minimum distance of -4.41 mm . The maximum distance corresponds to the distance of the stump that overlapped to socket (shown at the elbow region, dashed circle) while the minimum distance is the space created (shown at the bottom and at the right side views). Fig. 5e shows the chart showing the number of elements and the corresponding distance between the patient's stump and the socket. The mean distance is shown to be -0.46 mm ($SD = 1.70 \text{ mm}$) and the median distance is -0.35 mm . The concentration of the elements can be found at the zero distance because the volume of the stump and the socket were superimposed and were directly overlapping (cf. 5c). Depending on the patient's preference, liners will allow a snug-fitting socket. Commercially-available liners can be 2-4 mm in thickness. A liner with 3 mm thickness was provided to the patient (Icecross, item I-012426.5, Össur, Reykjavik, Iceland).

C. LINER FITTING AND PROSTHESIS ASSEMBLY

The liner, socket, and the cosmetic prosthetic arm were shipped to the patient. Fig. 6a shows the liner being worn by the patient. The threaded part was inserted through the socket to lock it using the shuttle lock ratchet. The full prosthetic arm assembly is shown in Fig. 6b. To remove the prosthetic arm, the shuttle lock button is pressed to release the thread. In Fig. 6c, the patient compared the length of the prosthetic arm with the non-affected arm. The shape and size of the prosthesis were compared with the uninjured hand at the volar (Fig. 6d) and dorsal sides (Fig. 6e).

D. PATIENT SATISFACTION SURVEY

The participant was asked to complete the OPUS self-report module on the Satisfaction with the Device [28]. On the question on appearance (i.e. My prosthesis looks good), she replied "neutral". On comfort-related questions below, the patient gave replies of "agree".

- My prosthesis fits well.
- It is easy to put on my prosthesis.
- My prosthesis is pain free to wear.

The method proposed in this work was able to address the issues related to comfort. While the shape and contours of the patient's arm were replicated with high accuracy, the patient mentioned that the coloration is also important for her; hence, she gave a neutral reply to the question on appearance. She said she would also have liked the prosthesis to be lighter in weight.

IV. DISCUSSION AND CONCLUSION

The loss of limbs due to war or accident creates a pronounced change in an individual's appearance. Such changes completely alter one's body image or one's perceptions, attitudes, beliefs, and dispositions toward one's own body [32]. A mismatch between one's ideal body and an altered body can create a negative body image resulting to negative effects on one's social skills [33], confidence and motivation [34]. Other reported effects are depression, feelings of hopelessness, feelings of low esteem, anxiety and sometimes suicidal thoughts [35]. Even when the mental and physical capacities to normally function are retained after amputation, some individuals still desire to make additional changes in their body to conceal or mask the loss of a body part [36].

The present work proposed a method for replicating the missing arm's shape and size that could be a step to address body image issues. The prosthetic arm was constructed by acquiring CT scans of the patient's affected and non-affected arms. The scanned data was digitally manipulated with Computer Aided Design software. The moulds were 3D printed and silicone material was used to cast the shape of the arm. Through these techniques, an accurate recreation of the amputated limb was made possible. For the arm, the Dice Similarity Coefficient (DSC) showed a result of 0.96, which indicate that the volume of the prosthetic arm is close to the volume of the mirrored image of the patient's uninjured arm.

The excess material corresponded to a 0.67% error in volume. This difference in volume corresponds to a maximum distance of 1.44 mm and a minimum of -2.17 mm in selected locations of the prosthetic arm. The central tendency indicators show that the mean distance between the prosthetic arm and the human arm is -0.34 mm ($SD = 0.48$ mm) and the median value is -0.32 mm. Both of these indicators approach 0 mm, implying a minimal difference in distance measures between the prosthetic arm and the human arm. For the socket, the DSC was 0.95 indicating that there is a close similarity when the stump was fitted with the open space in the socket. The volume of the stump that overlapped with the socket corresponded to a 2.97% error in volume. In terms of thickness, the overlap was reported to be 5.07 mm. However, other regions of the socket have available space for the displaced tissue to occupy. This corresponds to a distance of -4.41 mm from the stump to the available space at the wall of the socket. The mean distance between the socket and the stump is -0.46 mm ($SD = 1.70$ mm) and the median is -0.35 mm. Likewise, these values approach 0 mm, indicating that there is a minimal difference between the socket and the stump. With submillimeter resolutions of the CT scanners (Somatom, Siemens, Germany) and the 3D printer (Replicator 5th Generation, MakerBot Industries LLC, Brooklyn, NY, USA), the errors could be attributed to the errors in the design itself or to the shrinkage of the silicone material.

The design and fabrication methods described in the present work have distinct advantages over other traditional methods and over 3D printed designs. First, the patient has to visit the hospital once for a CT scan to be done. The patient does not have to get measured by the prosthetists or designers because the measurements are directly taken from the CT data. This approach allows the patient to be minimally exposed to the public. It was reported that those who lost limbs want to avoid unpleasant situations in public [37]. Second, there is no need for using digital photographs for scaling the prosthetic hands or arms. That approach can result in numerous errors from the depth of focus and lighting from the way the photos were taken. Designing the socket using the traditional approach would take several attempts to achieve acceptable results.

Lastly, the 3D printing fabrication method is highly suitable for one-off patient-specific prosthesis. There are different levels of amputation and there is no one-size-fits-all prosthesis. The associated direct cost of the materials and the consumed 3D printer filament was around \$20 for the arm. The socket and the liner costs \$960. These were more expensive because the materials selected ensured a more comfortable fit. When compared to the costs of high-technology prostheses (i.e. around \$4,000 to \$50,000), the incurred cost in our proposed method can make prostheses more affordable for underprivileged individuals. The affordable cost and the speed of production of 3D printing are suitable to create multiple prosthetic devices for a patient. For instance, the first prosthesis can be made immediately after the amputation, where a prosthesis can help lessen the impact of an altered

body image. The succeeding prostheses can serve other purposes that an amputee would prefer depending on his/her stage of coping. For example, one set of a patient's prosthetic arm might be aimed for better appearance while another would be more mechanical looking, which is aimed for activities of daily living or for sports.

Future work includes the reduction of weight of the prosthesis. From earlier studies by de Leva [38], it was estimated that a female with a body mass of 61.9 kg will have a combined forearm and hand mass of 2.23% of the body mass. The current patient has a body mass of 63.9 kg and by proportion, the patient's combined forearm and hand mass is approximately 2.3% of her body mass, which is around 1.47 kg. The prosthetic arm and socket have a combined mass of 1.06 kg as measured by a precision weighing scale (LPG-2102i, VWR Intl LLC, USA). Although the prosthesis is 27.89% lighter, reducing the mass further is possible because we have the ability to manipulate the geometry of the prosthesis; hence we can optimise the volume of the materials to be used. For instance, air pockets can be introduced in the design to increase the skin compliance while reducing material volume [36].

Affordability will make prosthetic devices part of an amputee's wardrobe. As technology advances and the costs reduce, the prosthetic arms that the amputees can have in the future can have features for social interactions. For example, some of the early prosthetics have embedded tactile sensors [39]–[42] or lifelike warmth [43], [44] and softness [45], [46], which are meant for perceiving touching and being touched. The present design lays the foundation for advancing 3D printed prosthetic arms and to which these embellishments can be provided in the future.

ACKNOWLEDGMENT

The authors are grateful to Amer Hawafdeh of Hamad Medical Corp, Doha, Qatar for the guidance in designing the socket moulds.

REFERENCES

- [1] *Guidelines for Training Personnel in Developing Countries for Prosthetics and Orthotics Services*, World Health Organization, Geneva, Switzerland, 2005.
- [2] *WHO Standards for Prosthetics and Orthotics*, World Health Organization, Geneva, Switzerland, 2017.
- [3] (2017). *World Population by Region*. [Online]. Available: <http://www.worldometers.info/world-population/#region>
- [4] Handicap International. (2015). *80,000 in Syria Need a Prosthesis or an Orthosis*. [Online]. Available: http://www.handicap-international.us/80_000_people_in_syria_need_a_prosthesis_or_an_orthosis
- [5] J. Kate, G. Smit, and P. Breedveld, "3D-printed upper limb prostheses: A review," *Disab. Rehabil., Assistive Technol.*, vol. 12, no. 3, pp. 300–314, 2017.
- [6] K. Takagishi and S. Umezu, "Development of the improving process for the 3D printed structure," *Sci. Rep.*, vol. 7, Jan. 2017, Art. no. 39852.
- [7] C. W. Hull, "Apparatus for production of three-dimensional objects by stereolithography," U.S. Patent 4 575 330, Mar. 11, 1986.
- [8] E. MacDonald et al., "3D printing for the rapid prototyping of structural electronics," *IEEE Access*, vol. 2, pp. 234–242, Dec. 2014.
- [9] C. Kim et al., "3D printed electronics with high performance, multi-layered electrical interconnect," *IEEE Access*, vol. 5, pp. 25286–25294, 2017.

- [10] G. P. Le Sage, "3D printed waveguide slot array antennas," *IEEE Access*, vol. 4, pp. 1258–1265, 2016.
- [11] Z. Li et al., "Processing and 3D printing of gradient heterogeneous bio-model based on computer tomography images," *IEEE Access*, vol. 4, pp. 8814–8822, 2016.
- [12] J. Shi, J. Yang, L. Zhu, L. Li, Z. Li, and X. Wang, "A porous scaffold design method for bone tissue engineering using triply periodic minimal surfaces," *IEEE Access*, vol. 6, pp. 1015–1022, 2017.
- [13] S. J. Lee, W. Zhu, L. Heyburn, M. Nowicki, B. Harris, and L. G. Zhang, "Development of novel 3-D printed scaffolds with core-shell nanoparticles for nerve regeneration," *IEEE Trans. Biomed. Eng.*, vol. 64, no. 2, pp. 408–418, Feb. 2017.
- [14] K. Schwab, *The Fourth Industrial Revolution*. Baltimore, MD, USA: Penguin, 2016.
- [15] E. Biddiss, D. Beaton, and T. Chau, "Consumer design priorities for upper limb prosthetics," *Disab. Rehabil. Assist. Technol.*, vol. 2, no. 5, pp. 346–357, 2007.
- [16] Open Bionics. (2017). *e-NABLE*. [Online]. Available: <http://www.openbionics.com>
- [17] (2017). *e-NABLE Community*. [Online]. Available: <http://enablingthefuture.org>
- [18] A. L. Muilenburg and M. A. LeBlanc, "Body-powered upper-limb components," in *Comprehensive Management of the Upper-Limb Amputee*. New York, NY, USA: Springer, 1989, pp. 28–38.
- [19] R. D. Alley and H. H. Sears, "Powered upper limb prosthetics in adults," in *Powered Upper Limb Prostheses*. Berlin, Germany: Springer, 2004, pp. 117–145.
- [20] A. Arabian, D. Varotsis, C. McDonnell, and E. Meeks, "Global social acceptance of prosthetic devices," in *Proc. IEEE Global Humanitarian Technol. Conf.*, Oct. 2016, pp. 563–568.
- [21] C. D. Murray, "The social meanings of prosthesis use," *J. Health Psychol.*, vol. 10, no. 3, pp. 425–441, 2005.
- [22] F. Cordella et al., "Literature review on needs of upper limb prosthesis users," *Frontiers Neurosci.*, vol. 10, p. 209, May 2016.
- [23] J.-J. Cabibihan, S. Pattofatto, M. Jomâa, A. Benallal, and M. C. Carrozza, "Towards humanlike social touch for sociable robotics and prosthetics: Comparisons on the compliance, conformance and hysteresis of synthetic and human fingertip skins," *Int. J. Social Robot.*, vol. 1, no. 1, pp. 29–40, 2009.
- [24] J.-J. Cabibihan, R. Pradipta, Y. Z. Chew, and S. S. Ge, "Towards humanlike social touch for prosthetics and sociable robotics: Handshake experiments and finger phalange indentations," in *Advances in Robotics (Lecture Notes in Computer Science)*, vol. 5744, J. H. Kim et al., Eds. Berlin, Germany: Springer, 2009, pp. 73–79.
- [25] J.-J. Cabibihan and S. S. Ge, "Towards humanlike social touch for prosthetics and sociable robotics: Three-dimensional finite element simulations of synthetic finger phalanges," in *Advances in Robotics (Lecture Notes in Computer Science)*, vol. 5744, J. H. Kim et al., Eds. Berlin, Germany: Springer, 2009, pp. 80–86.
- [26] M. E. L. Leow, R. W. H. Pho, and B. P. Pereira, "Esthetic prostheses in minor and major upper limb amputations," *Hand Clin.*, vol. 17, no. 3, pp. 489–497, 2001.
- [27] Touch Bionics. (2017). *LivingSkin Passive Functional Prosthesis*. [Online]. Available: <http://www.touchbionics.com>
- [28] A. W. Heinemann, R. K. Bode, and C. O'Reilly, "Development and measurement properties of the orthotics and prosthetics users' survey (OPUS): A comprehensive set of clinical outcome instruments," *Prosthetics Orthotics Int.*, vol. 27, no. 3, pp. 191–206, 2003.
- [29] S. Garrison, *Handbook of Physical Medicine and Rehabilitation Basics* (Lippincott Williams and Wilkins Handbook). Alphen aan den Rijn, The Netherlands: Wolters Kluwer, 2003.
- [30] *Prosthetics-Orthotics Thermoforming Polypropylene (Draping Technique)*, Int. Committee Red Cross, Geneva, Switzerland, 2015.
- [31] L. R. Dice, "Measures of the amount of ecologic association between species," *Ecology*, vol. 26, no. 3, pp. 297–302, 1945.
- [32] F. B. Mills, "A phenomenological approach to psychoprosthetics," *Disab. Rehabil.*, vol. 35, no. 9, pp. 785–791, 2013.
- [33] A. Bessell, E. Dures, C. Semple, and S. Jackson, "Addressing appearance-related distress across clinical conditions," *Brit. J. Nursing*, vol. 21, no. 19, pp. 1138–1143, 2012.
- [34] T. Green, "Understanding body image in patients with chronic oedema," *Brit. J. Community Nursing*, vol. 13, no. 10, p. S15–S18, 2008.
- [35] M. J. Hertenstein, D. Keltner, B. App, B. A. Bulleit, and A. R. Jaskolka, "Touch communicates distinct emotions," *Emotion*, vol. 6, no. 3, pp. 528–533, 2006.
- [36] J.-J. Cabibihan, R. Pradipta, and S. S. Ge, "Prosthetic finger phalanges with lifelike skin compliance for low-force social touching interactions," *J. NeuroEng. Rehabil.*, vol. 8, no. 1, pp. 1–16, 2011.
- [37] B. Bowers, "Providing effective support for patients facing disfiguring surgery," *Brit. J. Nursing*, vol. 17, no. 2, pp. 94–98, 2008.
- [38] P. de Leva, "Adjustments to Zatsiorsky-Seluyanov's segment inertia parameters," *J. Biomech.*, vol. 29, no. 9, pp. 1223–1230, 1996.
- [39] A. Chortos, J. Liu, and Z. Bao, "Pursuing prosthetic electronic skin," *Nature Mater.*, vol. 15, pp. 937–950, Jul. 2016.
- [40] W. W. Lee, J.-J. Cabibihan, and N. V. Thakor, "Bio-mimetic strategies for tactile sensing," in *Proc. IEEE SENSORS*, Nov. 2013, pp. 1–4.
- [41] A. Y. Alhaddad et al., "Toward 3D printed prosthetic hands that can satisfy psychosocial needs: Grasping force comparisons between a prosthetic hand and human hands," in *Social Robotics*, A. Kheddar et al., Eds. Cham, Switzerland: Springer, 2017, pp. 304–313.
- [42] J.-J. Cabibihan, S. S. Chauhan, and S. Suresh, "Effects of the artificial skin's thickness on the subsurface pressure profiles of flat, curved, and braille surfaces," *IEEE Sensors J.*, vol. 14, no. 7, pp. 2118–2128, Jul. 2014.
- [43] J.-J. Cabibihan, R. Jegadeesan, S. Salehi, and S. S. Ge, "Synthetic skins with humanlike warmth," in *Social Robotics*. Berlin, Germany: Springer, 2010, pp. 362–371.
- [44] J. J. Cabibihan, D. Joshi, Y. M. Srinivasa, M. A. Chan, and A. Muruganantham, "Illusory sense of human touch from a warm and soft artificial hand," *IEEE Trans. Neural Syst. Rehabil. Eng.*, vol. 23, no. 3, pp. 517–527, May 2015.
- [45] J.-J. Cabibihan, S. Pattofatto, M. Jomâa, A. Benallal, M. C. Carrozza, and P. Dario, "The conformance test for robotic/prosthetic fingertip skins," in *Proc. 1st IEEE/RAS-EMBS Int. Conf. Biomed. Robot. Biomechatronics (BioRob)*, Feb. 2006, pp. 561–566.
- [46] J.-J. Cabibihan, M. C. Carrozza, P. Dario, S. Pattofatto, M. Jomâa, and A. Benallal, "The Uncanny Valley and the search for human skin-like materials for a prosthetic fingertip," in *Proc. 6th IEEE-RAS Int. Conf. Humanoid Robots*, Dec. 2006, pp. 474–477.



JOHN-JOHN CABIBIHAN (SM'15) received the Ph.D. degree in bioengineering, with specialization in biorobotics, from the Scuola Superiore Sant'Anna, Pisa, Italy, in 2007, on scholarship grant. Concurrent with his Ph.D. studies, he received another scholarship grant from the École Normale Supérieure Paris-Saclay, France, in 2004. Therein, he spent one year at the Laboratoire de Mécanique et Technologie. From 2008 to 2013, he was an Assistant Professor with the Electrical and Computer Engineering Department, National University of Singapore, where he also served as a Deputy Director of the Social Robotics Laboratory and an Affiliate Faculty Member of the Singapore Institute of Neurotechnologies. He is currently an Associate Professor with the Mechanical and Industrial Engineering Department and a member of the Faculty Senate of Qatar University. He is a lead/co-lead principal investigator of several projects under the National Priorities Research Program of the Qatar National Research Fund. His research interests include: assistive and social robotics for the therapy of children with autism, life-like prosthetics, bio-inspired tactile sensing, and human-robotic touch and gestures. He was a General Chair of the 6th IEEE International Conference on Cybernetics and Intelligent Systems, Manila, 2013, a Program Chair of the International Conference on Social Robotics (ICSR) 2012, Chengdu, China, and ICSR 2016 Kansas City, USA, and a Program Co-Chair of ICSR 2010, Singapore, and ICSR 2017 Tsukuba, Japan. He serves on the Editorial Board of the *International Journal of Social Robotics*, the *International Journal of Advanced Robotics Systems*, *Frontiers in Bionics and Biomimetics*, *Frontiers in Special Education Needs*, and *Computational Cognitive Science*.



M. KHALEEL ABUBASHA received the B.Sc. degree in mechanical engineering from Qatar University in 2015. He is currently pursuing the Ph.D. degree with the Department of Mechanical Engineering, Texas A&M University, College Station, TX, USA. He was a Research Assistant with the Mechanical and Industrial Engineering Department, Qatar University, from 2015 to 2017. He is also a Graduate Research Assistant with the Department of Mechanical Engineering, Texas A&M University. His current research interests include the nanoscale tribology of skin, haptics, and neural systems for biomedical and industrial applications.



NITISH THAKOR (F'94-LF'17) has been a Professor of biomedical engineering with Johns Hopkins University since 1983. He has also been the Director of the Singapore Institute for Neurotechnology, National University of Singapore, and a Professor of electrical and computer engineering and biomedical engineering since 2012. His technical expertise is in the field of neuroengineering, where he has pioneered many technologies for brain monitoring to prosthetic arms and neuroprosthesis. He is a fellow of the American Institute of Medical and Biological Engineering, a Founding Fellow of the Biomedical Engineering Society, and a fellow of the International Federation of Medical and Biological Engineering. He was a recipient of the Research Career Development Award by the National Institutes of Health, the Presidential Young Investigator Award by the National Science Foundation, the Academic Career Award and the Technical Excellence in Neuroengineering by the IEEE Engineering in Medicine and Biology Society, the Distinguished Alumnus Award by IIT, Bombay, India, and the Centennial Medal by the School of Engineering, University of Wisconsin. He was the Editor-in-Chief of IEEE TNSRE from 2005 to 2011. He is currently the Editor-in-Chief of *Medical and Biological Engineering and Computing*.

• • •